

Medium Modifications of Hadron Properties and Partonic Processes

W. K. Brooks¹, S. Strauch² and K. Tsushima³

¹ Universidad Técnica Federico Santa María, Valparaíso, Chile

² University of South Carolina, Columbia, South Carolina 29208, USA

³ University of Adelaide, South Australia 5005, Australia

Abstract. Chiral symmetry is one of the most fundamental symmetries in QCD. It is closely connected to hadron properties in the nuclear medium *via* the reduction of the quark condensate $\langle \bar{q}q \rangle$, manifesting the partial restoration of chiral symmetry. To better understand this important issue, a number of Jefferson Lab experiments over the past decade have focused on understanding properties of mesons and nucleons in the nuclear medium, often benefiting from the high polarization and luminosity of the CEBAF accelerator. In particular, a novel, accurate, polarization transfer measurement technique revealed for the first time a strong indication that the bound proton electromagnetic form factors in ^4He may be modified compared to those in the vacuum. Second, the photoproduction of vector mesons on various nuclei has been measured *via* their decay to e^+e^- to study possible in-medium effects on the properties of the ρ meson. In this experiment, no significant mass shift and some broadening consistent with expected collisional broadening for the ρ meson has been observed, providing tight constraints on model calculations. Finally, processes involving in-medium parton propagation have been studied. The medium modifications of the quark fragmentation functions have been extracted with much higher statistical accuracy than previously possible.

1. Introduction

One of the most exciting topics in nuclear physics is to study how the properties of hadrons are modified by the nuclear environment, and how such modifications are related to the properties of nuclei and nuclear phenomena. Since nucleons and mesons are made of quarks, antiquarks and gluons, one expects their internal structure to be modified when placed in a nuclear medium or atomic nuclei [1]. From the QCD point of view, this is primarily the manifestation of modifications of the quark condensate in the nuclear medium, which is closely associated with the partial restoration of chiral symmetry. Similarly, medium modifications of partonic processes are directly tied to the gluon density of the medium. The modern view of the nucleus must inescapably include these ingredients, which come directly from the properties of the QCD Lagrangian.

There is little doubt that, at sufficiently high nuclear density and/or temperature, quarks and gluons are the correct degrees of freedom. By contrast, the general success of conventional nuclear physics (with *effective* interactions) indicates that nucleons and mesons provide a good starting point for describing a nucleus at low energy. Therefore, a consistent nuclear theory describing the transition from nucleon and meson degrees of freedom to quarks and gluons is truly required to describe nuclei and nuclear matter over a wide range of density and temperature. Of course, theoretically, lattice QCD simulations may eventually give reliable information on

the density and temperature dependence of hadron properties in the nuclear medium. However, current simulations have just started to study the 2-body, nucleon-nucleon [2] and nucleon-hyperon interactions [3], which is still very far from what is needed for the description of a finite nucleus. At present, although one is forced to rely on some models, it is a very important step to understand the main features of nuclear phenomena and the structure of finite nuclei based on the quark and gluon degrees of freedom [4].

We know that explicit quark degrees of freedom are certainly necessary to understand deep-inelastic scattering (DIS) at momentum transfers of several GeV. In particular, the nuclear EMC effect [5] has suggested that it is vital to include some dynamics beyond the conventional nucleon-meson treatment of nuclear physics to explain the nuclear structure function data [6, 7]. This leads to the extraction of nuclear parton, or bound-nucleon parton distributions [8, 9]. In-medium structure functions were studied at Jefferson Lab in an EMC-type experiment in heavy nuclei, emphasizing the large- x region [10, 11], and recently also in few-body nuclei [12, 13]. Another series of Jefferson Lab experiments focus on the longitudinal-transverse separation of in-medium structure functions [14, 15].

Furthermore, the search for evidence of some modification of nucleon properties in medium has recently been extended to the nucleon electromagnetic form factors in polarized ($\vec{e}, e'\vec{p}$) scattering experiments on ^{16}O [16, 17] and ^4He [18, 19, 20, 21, 22] nuclei at MAMI and Jefferson Lab. These experiments observed the double ratio of proton-recoil polarization transfer coefficients in the scattering off nuclei with respect to the elastic $^4\text{He}(\vec{e}, e'\vec{p})$ reaction at four-momentum transfers squared of several 100 $(\text{MeV}/c)^2$ to a few $(\text{GeV}/c)^2$. The results from ^4He strongly hint at the need to include medium modifications of the proton electromagnetic form factors. The recent Coulomb sum rule experiment at Jefferson Lab [23] is a precision measurement of response functions in quasi-elastic electron scattering and will provide important data on the nucleon charge properties in the nuclear medium, providing important constraints on the electric form factor of the proton.

The photoproduction of vector mesons on various nuclei has been studied to search for possible in-medium modifications of the vector-meson spectral functions. The vector mesons, ρ , ω , and ϕ , are observed *via* their decay to e^+e^- , in order to reduce the effects of final state interactions in the nucleus [24, 25, 26]. However, in these experiments mesons measured were moving relatively fast. In-medium modifications at lower momenta have not yet been observed experimentally. One can expect that the quarks inside the fast moving mesons do not have enough time to adjust to the surrounding nuclear medium. Thus, further experiments with nearly stopped meson kinematics are certainly required to draw more concrete conclusions.

Another interesting class of medium modifications consists of the changes in fundamental partonic processes that are embedded in the medium. The well-established features of quark fragmentation in vacuum are strongly modified in the cold nuclear medium, a topic best addressed in semi-inclusive DIS on nuclei. A second effect is the alteration of the process whereby a highly virtual quark radiates gluons, leading to an increased rate of energy loss. Precise characterization of these effects in the cold medium, in addition to giving new insight into QCD, may also aid interpretation of observables in the hot medium. These medium modifications of fundamental partonic vacuum processes are now beginning to be understood theoretically after more than two decades of investigation.

In this article, the medium modifications of nucleon structure, electromagnetic form factors and structure functions are focused on in Section 2, while the modifications of meson structure, masses and widths are focused on in Section 3. Section 4 treats the medium modification of partonic processes, discussing modification of fragmentation functions and medium-induced quark energy loss. An overview of experiments at Jefferson Lab, dedicated to the study of medium modifications of both nucleon and meson properties, is given in Table 1.

Table 1. Jefferson Lab experiments to study medium modifications.

In-medium property	Reaction	Target	Exp. proposals
Form factors	$(\vec{e}, e'\vec{p})$	$^1\text{H}, ^2\text{H}, ^4\text{He}, ^{16}\text{O}$	[27, 19, 20, 16]
Nucleon charge	(e, e')	$^4\text{He}, ^{12}\text{C}, ^{56}\text{Fe}, ^{208}\text{Pb}$	[23]
Structure function F_2	(e, e')	$^1\text{H}, ^2\text{H}, ^3\text{He}, ^4\text{He}, \text{Be}, \text{C},$ Al, Fe, Cu, Au	[10, 11, 12]
Structure functions $F_2, \sigma_L/\sigma_T$	(e, e')	$^1\text{H}, ^2\text{H}, \text{C}, \text{Al}, \text{Fe}$	[14, 15]
Vector-meson spectral functions	(γ, e^+e^-)	$^2\text{H}, ^{12}\text{C}, \text{Fe-Ti}$	[24]
Fragmentation functions, Δp_T	$(e, e'X)$	$^2\text{H}, \text{C}, \text{Al}, \text{Fe}, ^{120}\text{Sn}, \text{Pb}$	[28]

2. Nucleon structure modification

2.1. Modification of electromagnetic form factors

2.1.1. In-medium form factors

Whether the nucleon changes its fundamental properties while embedded in a nuclear medium has been a long-standing question in nuclear physics, attracting experimental and theoretical attention. QCD is established as the theory of the strong nuclear force but the degrees of freedom observed in nature, hadrons and nuclei, are different from those appearing in the QCD Lagrangian, quarks and gluons. There are no calculations available for nuclei within the QCD framework. Nuclei are effectively and well described as clusters of protons and neutrons held together by a strong, long-range force mediated by meson exchange [29].

Distinguishing possible changes in the structure of nucleons embedded in a nucleus from more conventional many-body effects like meson exchange currents (MEC), isobar configurations (IC) or final state interactions (FSI) is only possible within the context of a model. Therefore, interpretation of an experimental signature as an indication of nuclear medium modifications of the form factors is better motivated if this results in a more economical description of the nuclear many-body system. In this context, a calculation by Lu *et al.* [30], using a quark-meson coupling (QMC) model, suggests a measurable deviation from the free-space electromagnetic form factor over the four-momentum transfer squared Q^2 range $0 < Q^2 < 2.5$ (GeV/c) 2 . Similar measurable effects have been calculated in a light-front constituent quark model by Frank *et al.* [31], a modified Skyrme model by Yakshiev *et al.* [32], a chiral quark soliton model (CQS) by Smith and Miller [33], and the Nambu-Jona-Lasinio model of Horikawa and Bentz [34]. Medium modifications of nucleon properties in nuclear matter and finite nuclei have been also discussed by Wen and Shen [35]. Furthermore, the nuclear modification of axial form factors [36] also may be measured.

The connection between the modifications induced by the nuclear medium of the nucleon form factors and of the deep inelastic structure functions was discussed by Liuti [37] using the concept of generalized parton distributions (GPDs). Guzey *et al.* [38] have studied incoherent deeply virtual Compton scattering (DVCS) on ^4He in the $^4\text{He}(e, e'\gamma p)X$ reaction, which probes medium modifications of the bound nucleon GPDs and elastic form factors. They have also investigated medium modification of the quark contribution to the spin sum rule [39]. The relation between the medium modified form factors and structure functions was also discussed in Ref. [40] in the framework of quark-hadron duality, where the size of the medium modification in the former was used to place constraints on models of the nuclear EMC effect which assume a large deformation of the intrinsic structure of the nucleon in medium.

The best experimental constraints on the changes in the electromagnetic form factors come from the analysis of y -scaling data. For example, in the iron nucleus (Fe) the nucleon root-mean-square radius cannot vary by more than 3% [41]. However, in the kinematic range covered by this y -scaling analysis, the eN cross section is predominantly magnetic, so this limit applies

essentially to G_M . (As the electric and magnetic form factors contribute typically in the ratio 1:3 the corresponding limit on G_E would be nearer 10%.) For the QMC model, the calculated increase in the root-mean-square radius of the magnetic form factors is less than 0.8% at ρ_0 [30]. For the electric form factors the best experimental limit seems to come from the Coulomb sum-rule, where a variation bigger than 4% would be excluded [42]. This is similar in size to the variations calculated in the QMC model (*e.g.*, 5.5% for G_E^p at ρ_0) [30] and not sufficient to reject them.

2.1.2. Medium modifications from recoil polarization experiments One of the most intuitive methods to investigate the properties of nucleons inside nuclei is quasi-elastic scattering off nuclei. Since the charge and magnetic responses of a single nucleon are quite well studied from elastic scattering experiments, measuring the same response from quasi-elastic scattering off nuclei and comparing with a single nucleon is likely to shed light on the question. The polarization transfer ratio in elastic $\vec{e}p$ scattering, P'_x/P'_z , is directly proportional to the ratio of the electric and magnetic form factors of the proton [43]; here P'_x and P'_z are the polarization transfer observables transverse and longitudinal to the momentum transfer direction. When such measurements are performed on a nuclear target in quasi-elastic kinematics, the polarization transfer observables are sensitive to the form factor ratio of the proton embedded in the nuclear medium. Experimental results for the polarization transfer ratio are conveniently expressed in terms of the polarization double ratio

$$R = \frac{(P'_x/P'_z)_A}{(P'_x/P'_z)_{\text{1H}}}, \quad (1)$$

in order to emphasize differences between the in-medium and free values. Here the polarization transfer ratio for the quasi-elastic proton knockout $A(\vec{e}, e'\vec{p})$ reaction is normalized to the hydrogen polarization transfer ratio measured in the identical setting. Such a double ratio cancels nearly all experimental systematic uncertainties.

Experiment E89-033 was the first to measure the polarization transfer in a complex nucleus, ^{16}O [17]. The results are consistent with predictions of relativistic calculations based on the free proton form factor with an experimental uncertainty of about 18%. Earlier polarization transfer experiments have studied nuclear medium effects in deuterium [44, 45, 46] at the Mainz microtron (MAMI) and MIT-Bates. More recently, polarization transfer data on ^2H were measured in Jefferson Lab experiment E89-028 [47]. The data are shown in Fig. 1 and compared with a model calculation by Arenhövel, which includes final state interactions, meson exchange currents, and isobar configurations, as well as relativistic contributions (RC) of leading order in p/m_N to the kinematic wave function boost and to the nucleon current. Arenhövel's calculation describes the ^2H data well. Within statistical uncertainties, no evidence of medium modifications is found. As the sampled nuclear density is small and the bound proton is nearly on-shell in the kinematics of this experiment, it is not surprising that there are no indications for medium modifications of the proton electromagnetic form factors in the ^2H data.

One might expect to find larger medium effects in ^4He , with its significantly higher density. Although estimates of the many-body effects in ^4He may be more difficult than in ^2H , calculations for ^4He indicate they are small [48]. The first $^4\text{He}(\vec{e}, e'\vec{p})^3\text{H}$ polarization transfer measurements were performed at MAMI at $Q^2 = 0.4$ (GeV/c) 2 [18] and at Jefferson Lab Hall A at $Q^2 = 0.5, 1.0, 1.6,$ and 2.6 (GeV/c) 2 , E93-049 [21]. Experiment E03-104 extended these measurements with two high-precision points at $Q^2 = 0.8$ and 1.3 (GeV/c) 2 [22]. All these data were taken in quasi-elastic kinematics at low missing momentum with symmetry about the three-momentum transfer direction to minimize conventional many-body effects in the reaction. The missing-mass technique was used to identify ^3H in the final state.

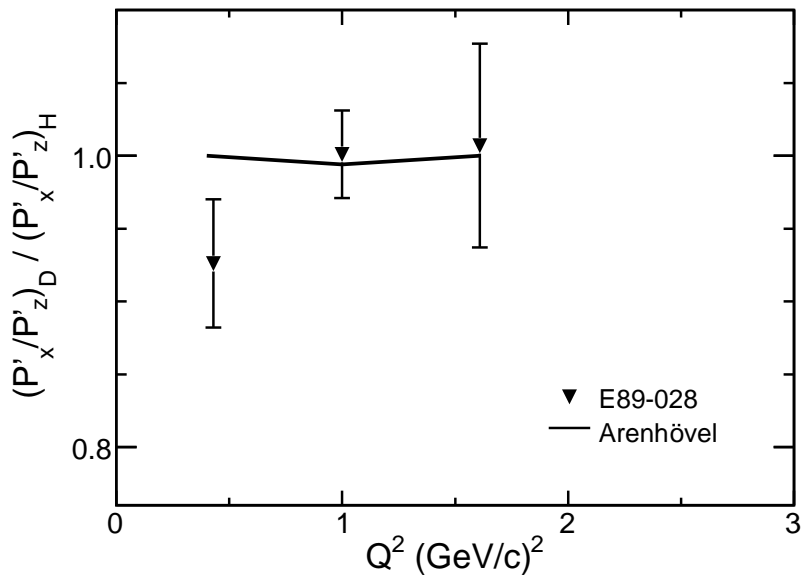


Figure 1. Bound-to-free polarization transfer double ratio R for ${}^2\text{H}(\vec{e}, e'\vec{p})n$ (triangles) from [47] as a function of Q^2 . The curve shows results of a calculation by Arenhövel; see [47].

The ${}^4\text{He}$ polarization transfer double ratio is shown in Figure 2. The new data from E03-104 [22] are consistent with the previous data from E93-049 [21] and MAMI [18]. The polarization transfer ratio (P'_x/P'_z) in the $(\vec{e}, e'\vec{p})$ reaction on helium is significantly different from those on deuterium or hydrogen. The helium data are compared with results of a relativistic distorted-wave impulse approximation (RDWIA) calculation by the Madrid group [49, 50] (dotted curve). In this model FSI are incorporated using relativistic optical potentials that distort the final nucleon wave function. MEC are not explicitly included in the Madrid calculation. Predictions by Meucci *et al.* [51] show that the two-body current (the seagull diagram) effects are generally small (less than 3% close to zero missing momenta) and visible only at high missing momenta. It can be seen that the Madrid RDWIA calculation (dotted curve) overestimates the data by about 6%. The calculations shown uses the Coulomb gauge, the $cc1$ and $cc2$ current operators as defined in [52], and the MRW optical potential of [53]. The $cc1$ current operator gives lower values of R than the $cc2$ operator. In general, various choices for, *e.g.*, spinor distortions, current operators, and relativistic corrections affect the theoretical predictions by $\leq 3\%$ within the RDWIA model, and presently cannot explain the disagreement between the data and the RDWIA calculation. We note that these relativistic calculations provide good descriptions of, *e.g.*, the induced polarizations as measured at Bates in the ${}^{12}\text{C}(e, e'\vec{p})$ reaction [54, 50] and of A_{TL} in ${}^{16}\text{O}(e, e'p)$ as previously measured at Jefferson Lab [55]. After including the density-dependent medium-modified form factors from the QMC [30] or CQS [33] models in the RDWIA calculation (solid and dashed curves), good agreement with the polarization transfer data is obtained.

This agreement has been interpreted as possible evidence of proton medium modifications [21]. This interpretation is based on the description of the data in a particular model in terms of medium modifications of nucleon form factors and requires excellent control of the reaction mechanisms such as meson exchange currents, isobar configurations, and final state interactions. In fact, there is an alternative interpretation of the observed suppression of the polarization transfer ratio within a more traditional calculation by Schiavilla *et al.* [56] (shaded band). The latter calculation uses free nucleon form factors and explicitly includes MEC effects

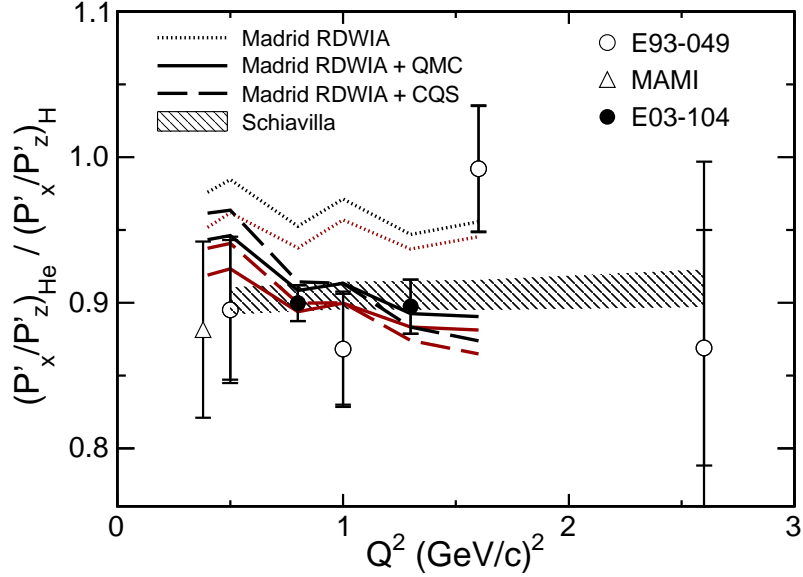


Figure 2. $^4\text{He}(\vec{e}, e'\vec{p})^3\text{H}$ polarization transfer double ratio R as a function of Q^2 from Mainz [18] and Jefferson Lab experiments E93-049 [21] (open symbols) and E03-104 [22] (filled circles). The data are compared to calculations from Schiavilla *et al.* [56] and the Madrid group [49, 50] using the *cc1* (lower set of curves) and *cc2* (upper set of curves) current operators. In-medium form factors from the QMC [30] (solid curves) and CQS [33] (dashed curves) models were used in two of the Madrid calculations. Not shown are a relativistic Glauber model calculation by the Ghent group [57] and results from Laget [48] which give both a value of $R \approx 1$.

which suppress R by almost 4%. The FSIs are treated within the optical potentials framework and include both a spin-dependent and spin-independent charge-exchange term; the spin-orbit terms, however, are not well constrained by data. In the model of Schiavilla *et al.*, the final state interaction effects suppress R by an additional 6% bringing this calculation also in good agreement with the data within the statistical uncertainties associated with the Monte Carlo technique in this calculation. It should be noted that charge-exchange terms are not taken into account in the Madrid RDWIA calculation. The difference in the modeling of final state interactions is the origin of the major part of the difference between the results of the calculations by Udias *et al.* [49, 50] and Schiavilla *et al.* [56] for the polarization observables.

Effects from final state interactions can be studied experimentally with the induced polarization, P_y , which is a direct measure of final state interactions. Induced-polarization data were taken simultaneously to the polarization transfer data. Figure 3 shows the data for P_y . The induced polarization is small at the low missing momenta in this reaction. The sizable systematic uncertainties are due to possible instrumental asymmetries. Dedicated data have been taken during E03-104 to study these and work is underway to significantly reduce the systematic uncertainties in P_y in the final analysis. The data are compared with the results of the calculations from the Madrid group and Schiavilla *et al.* at missing momenta of about zero. To facilitate this comparison, the data have been corrected for the spectrometer acceptance. The preliminary data suggest that the induced polarization (and thus the final state interaction) is underestimated in the MRW optical potential in the model of the Madrid group and overestimated in the model of Schiavilla *et al.* Note that the charge-exchange terms, particularly the spin-dependent one, gives the largest contribution to P_y in the Schiavilla *et al.*

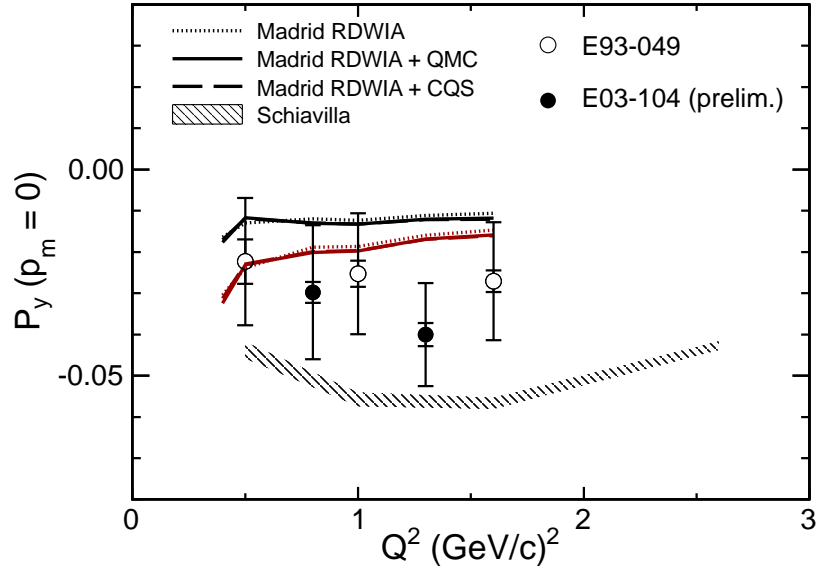


Figure 3. Induced polarization data from Jefferson Lab experiment E93-049 [21] along with preliminary results from experiment E03-104 [58]. The data are compared to calculations from the Madrid group [49, 50] and Schiavilla *et al.* [56] as in Fig. 2. Note that the comparison is made for missing momentum $p_m \approx 0$; the experimental data have been corrected for the spectrometer acceptance for this comparison.

calculation. The induced polarization proves to be sensitive to the choice of optical potential allowing this observable to be used to constrain theoretical models of FSI. A comparison of the model calculations in Figure 2 and Figure 3 shows that the in-medium form factors mostly affect the ratio of polarization transfer observables and to a lesser extent the induced polarization. It is a great advantage of E03-104 to have access to both the polarization transfer and the induced polarization.

In summary, polarization transfer in the quasi-elastic ($e, e'p$) reaction is sensitive to possible medium modifications of the bound-nucleon form factor, while at the same time largely insensitive to other reaction mechanisms. Currently, the ${}^4\text{He}(\vec{e}, e'\vec{p}){}^3\text{H}$ polarization transfer data can be well described by either the inclusion of medium-modified form factors or strong charge-exchange FSI in the models. The analysis of the new high-precision induced-polarization data from Jefferson Lab Hall A has recently been finalized and the results provide now a more stringent test of these calculations [59].

2.1.3. Coulomb sum rule Experimental constraints on possible proton medium modifications are available for the electric form factor G_E from tests of the Coulomb sum rule (CSR) in quasi-elastic electron scattering off nuclei. This sum rule states that at large enough three-momentum transfer q the integration of the charge response $R_L(q, \omega)$ of a nucleus over the full range of energy loss ω , excluding the elastic peak at the lower limit, should be equal to the total charge Z of the nucleus [60]

$$S_L(q) = \frac{1}{Z} \int_{0^+}^{\infty} \frac{R_L(q, \omega)}{\tilde{G}_E^2} d\omega, \quad (2)$$

where $\tilde{G}_E = (G_E^p + (N/Z)G_E^n)\zeta$ takes into account the nucleon charge form factors and a relativistic correction, ζ . Pauli blocking at very small momentum transfer as well as short- and long-range correlations at medium and larger momentum transfer result in a quenching of the Coulomb sum rule. However, at sufficiently high momentum transfer, only short range correlation effects remain. They have been estimated by various theoretical calculations using different NN forces and found to be responsible for at most 10% quenching of the CSR integral. As a result, any further quenching of this quantity at sufficiently high momentum transfer may indicate the possibility of modified properties of the nucleon inside the nucleus [61].

Starting from this quite simple idea, for the past 20 years, various laboratories around the world performed experiments in diverse conditions, but the final conclusion is still controversial: on ${}^4\text{He}$, good agreement between theory and experiment is obtained when using free-nucleon form factors [62] and similar results were obtained on ${}^{12}\text{C}$ and ${}^{56}\text{Fe}$ [42]. However, a re-examination of the extraction of the longitudinal and transverse response functions on medium-weight and heavy nuclei (${}^{40}\text{Ca}$, ${}^{48}\text{Ca}$, ${}^{56}\text{Fe}$, ${}^{197}\text{Au}$, ${}^{208}\text{Pb}$ and ${}^{238}\text{U}$) in the framework of the Effective Momentum Approximation showed quenching of the Coulomb sum rule [60, 61]. This quenching corresponds to a relative change of the proton charge radius of $13 \pm 4\%$ and it was interpreted as an indication for a change of the nucleon properties inside the nuclear medium.

Jefferson Lab Experiment E05-110 is a precision test of the Coulomb sum rule [23]. The experiment measured the inclusive electron scattering cross sections off ${}^4\text{He}$, ${}^{12}\text{C}$, ${}^{56}\text{Fe}$, and ${}^{208}\text{Pb}$ in the quasi-elastic region and will make it possible to study A - or density-dependent effects of the CSR. The measurement covered a wide range of momentum transfers, $0.55 \text{ GeV}/c \leq q \leq 0.9 \text{ GeV}/c$, and thereby expanded the rather limited coverage of previous experiments. This measurement will provide data on the saturation or quenching of the Coulomb sum rule in a kinematic region where a clean access of the nucleon charge properties in the nuclear medium is plausible, free from Pauli blocking and long range correlations. Also, in this region short-range correlations are found to explain less than 10% reduction from the naive Coulomb sum rule. The kinematic range of the experiment overlaps with previous experiments at the low- q side and it provides a unique opportunity to investigate the q evolution of the Coulomb sum from the nucleonic to sub-nucleonic scale. Improved control of systematic uncertainties is possible through the measurement of quasi-elastic scattering cross sections at four different angles, providing four virtual photon polarization values ϵ at almost equal spacing. Two additional ϵ settings will provide a tool to study the effect of the Coulomb corrections. Also, the use of two different thicknesses for ${}^{208}\text{Pb}$ target will help to reduce any systematic errors from the radiative corrections. Data taking was completed in early 2008 and the analysis of the data, particularly the extraction of the longitudinal and transverse response functions, is underway.

2.2. Modification of unpolarized structure functions

The European Muon Collaboration (EMC) measured the ratios of structure functions of iron and deuterium in deep-inelastic scattering and found a reduction of the structure function of a nucleus compared to that of a free nucleon at intermediate values of Bjorken x , $0.3 < x < 0.6$. These measurements provided the first clear evidence that the quark structure of nucleons and nuclei were significantly different. Indeed, the nucleon bound in a nucleus carries less momentum than in free space. However, the specific causes of the modifications observed in nuclear structure functions have not yet been identified with certainty [63]. Although the simple kinematic effects of binding energy and Fermi motion do not account for the EMC effect [63], they do play a significant role at large x and are for those kinematics important in understanding the modification of the nuclear quark distributions [64]. A detailed study of these effects, however, is hindered by limited data. Most of the data are available only for heavy nuclei, yet few-body nuclei have the advantage that exact calculations are available. Particularly, uncertainties in the effect of binding due to uncertainties in the nuclear structure are reduced. Calculations also

predict large differences in both the magnitude and x dependence of the EMC effect in ^3He and ^4He , whereas the effect in various heavy nuclei show the same x dependence. The study of few-body nuclei can thus help to shed more light on the EMC effect. Data are furthermore sparse above $x = 0.8$, where binding and other short-distance effects should dominate. The F_2 structure function in inclusive electron scattering off nuclei at large Q^2 has been measured at Jefferson Lab Hall C in a series of experiments: E89-008 [10], E02-019 [11], and most recently in E03-103 [12]. The latter will provide better constraints on the effect of binding in the large- x region.

Jefferson Lab Experiment E03-103 provides a precision measurement of the EMC effect in both few-body nuclei and heavy nuclei. The experiment ran in 2004 in Hall C and measured inclusive electron scattering from ^1H , ^2H , ^3He , and ^4He as well as Be, C, Al, Cu, and Au over a broad range of x ($0.3 < x < 1.0$) up to $Q^2 \approx 8.0 \text{ GeV}^2$. The ^3He structure function was measured at x larger than 0.5 for the first time. Results from E03-103 along with previous SLAC results are shown in Fig. 4 [13]. The Jefferson Lab data are in good agreement with these previous

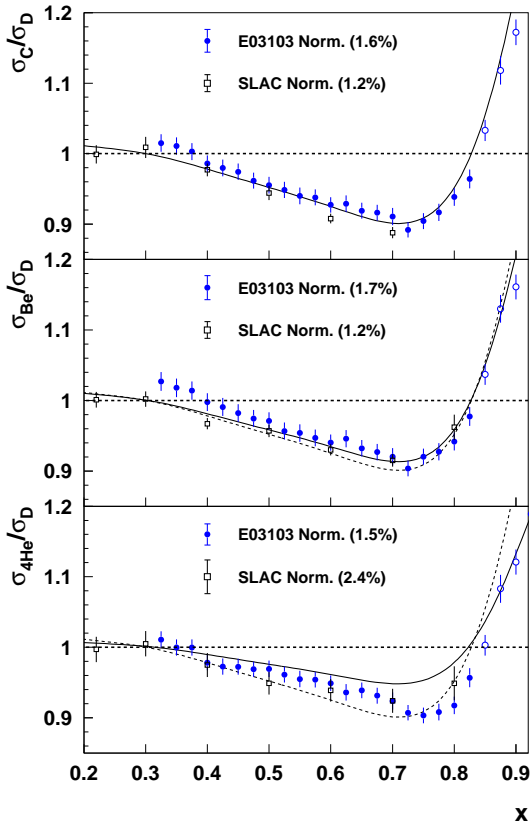


Figure 4. EMC cross-section ratios for ^{12}C (top), ^9Be , and ^4He from E03-103 [13] and SLAC [65]. The ^9Be results include a correction for the neutron excess (see [13]). Filled (open) circles denote W^2 above (below) 4 GeV^2 . The solid curve is the A -dependent fit to the SLAC data, while the dashed curve is the fit to ^{12}C . Normalization uncertainties are shown in parentheses for both measurements. Figure taken from [13].

results and improve significantly the precision of the EMC ratio at larger x . The findings of E03-103 indicate that the nuclear dependence of the cross section is comparable for ^4He , ^9Be , and ^{12}C (dashed curve); whereas the observed nuclear effects are clearly smaller for ^3He (not shown). The data thus do not support previous A -dependent fits to the EMC effect nor fits dependent on the *average* nuclear density. The average nuclear density is relatively low in ^9Be . The results rather suggest that the nuclear dependence of the quark distributions may depend on the *local* nuclear environment. The better coverage at larger x was achieved by relaxing the

usual W^2 cut for deep inelastic scattering from 4 GeV² down to below 2 GeV² after previous data showed that the structure function scales also at lower values of W (quark-hadron duality) [66]. Specific data were taken to verify this assumption. Data from E02-019 will further allow a detailed study of the scaling of nuclear structure functions in the $x > 1$ region.

Several experiments in Hall C measured the longitudinal-transverse separated structure functions F_2 and the ratio $R = \sigma_L/\sigma_T$ from nuclear targets at $Q^2 < 4$ (GeV/c)² [14, 15]. The data on R for hydrogen and deuterium have been published [67], and the data on the heavier targets are being analyzed. When fully available, these data will greatly increase our understanding of nuclear effects.

2.3. Modification of polarized structure functions

The well-known EMC effect has fascinated a generation of physicists and has stimulated much theoretical work. There is little question that the explanation of this phenomenon involves the modification of hadron structure in the medium, although the details of the descriptions vary. It is then to be expected that there may be an analogous change in the *spin* structure of the nucleon as well. Detailed calculations support this conjecture [68] and suggest that the observable modification is frequently larger than the unpolarized EMC effect.

Letters of intent have proposed measurements at 6 GeV [69, 70], however, the best measurement will be performed with the upgraded 12 GeV Jefferson Lab accelerator due to improved kinematic reach and better control of systematic uncertainties. The foundation that provides confidence that these studies can be realized is the large and successful Jefferson Lab program of polarized target studies on ¹H, ²H, and ³He described elsewhere in this document.

The method requires polarizing a nuclear target that is chosen to satisfy the following conditions:

- a large fraction of the overall nuclear polarization is concentrated on one nucleon within the nucleus;
- reliable calculations can be performed of the degree of polarization for the highly polarized nucleon;
- sufficient nuclear size to provide a medium environment representative of larger nuclei, while still limiting the dilution factor.

One example of a nucleus that satisfies these conditions is ⁷Li, for which detailed nuclear structure calculations exist [71, 72]. Asymmetry measurements can constrain the value of the medium-modified g_1 to the few-percent level over the range of interest in x_B from 0.05 to more than 0.5.

3. Meson structure modification

The masses of hadrons are created dynamically and are much larger than the summed masses of their constituents. The generation of hadronic masses is connected to spontaneous breaking of chiral symmetry and in-medium hadron properties, such as their masses and widths, are expected to change with chiral symmetry restoration. Various theoretical models predict an at least partial restoration of chiral symmetry at high temperatures and/or densities. By using effective chiral Lagrangians with a suitable incorporation of the scaling property of QCD, Brown and Rho [1] derived approximative in-medium scaling laws and predict for the ratio of vector-meson masses at nuclear-matter density, ρ_0 , compared to their free values $m^*(\rho_0)/m \approx 0.80$. Using QCD sum rules, Hatsuda and Lee [73] obtained the density dependence of this ratio, $m^*(\rho)/m \approx 1 - \alpha(\rho/\rho_0)$, with $\alpha = 0.18 \pm 0.06$. Models based on nuclear many-body effects predict a broadening in the width of the ρ meson with increasing density. This prediction is based on the assumption that many-body excitations may be present with the same quantum

numbers and can mix with the hadronic states [74, 75, 76, 77, 78, 79]. Furthermore, due to the uncertainty of the coupling constants as a function of density, the branching ratios are expected to change in the nuclear medium and also distort the invariant mass spectrum of the resonance [80].

First experimental studies of the properties of vector mesons as a function of temperature and density were done in relativistic and ultra-relativistic heavy-ion reactions. The CERES collaboration at CERN performed pioneering investigations of possible ρ -meson medium modifications through e^+e^- pair production in nucleus-nucleus collisions. A di-lepton yield exceeding expectations from hadron decays has been observed in the mass region 0.2 to 0.6 GeV/c². An upgraded CERES experiment with improved mass resolution confirmed these results, and found in addition a substantial in-medium broadening of the ρ spectral function over a density dependent shift of the ρ pole mass [81]. The result of $\mu^+\mu^-$ measurements in In-In collisions in the NA60 experiment at CERN has also shown a considerable broadening (doubling of the width) of the ρ spectrum, while no shift in the mass was observed [82, 83, 84]. In these heavy-ion reactions the temperature and/or density is varied and they proceed far from equilibrium under difficult to separate reaction mechanisms. This makes an interpretation of these results in terms of the chiral symmetry structure of the vacuum very challenging.

Medium modifications of mesons at zero temperature and normal nuclear matter density are experimentally accessible in photonuclear or elementary hadronic reactions on heavy nuclei. The best approach, free of final state interactions, is the study of the leptonic decay channel of these mesons. An observation of a medium-modified vector meson invariant mass decrease ($\alpha = 0.09 \pm 0.002$) has been claimed by a KEK-PS collaboration in an experiment where 12 GeV protons were incident on nuclear targets, and the e^+e^- pairs were detected [85, 86, 87]. The Crystal Barrel/TAPS collaboration has reported a 14% downward shift in the mass of the ω , where the analysis focused on the $\pi^0\gamma$ decay of *low-momentum* ω mesons photoproduced on a nuclear target [88]. However, in a recent re-analysis of these data the earlier claim of an in-medium mass shift of the ω could not be confirmed [89]. It is predicted that the ω potential in nuclear matter is attractive and possible to form nuclear bound state [90, 91, 92], if it is produced nearly with zero momentum.

The Jefferson Lab Experiment E01-112 studied the photoproduction of light vector mesons (ρ , ω , and ϕ) on deuterium and the heavier targets of carbon, titanium, and iron [24] with the CEBAF Large Acceptance Spectrometer (CLAS) [93]. The photon beam from the Hall B photon tagging facility covered an energy range from about 0.6 to 3.8 GeV. The CLAS has an excellent electron/pion discrimination, which allowed detection of the vector mesons *via* their rare leptonic decay in the e^+e^- channel and thus avoiding the complications from final state interactions of the hadronic decay channels.

The experimental e^+e^- invariant mass distribution includes the spectral distribution from the decay of the vector mesons ρ , ω , and ϕ . It also contains background from other physical processes, for example meson decays into γe^+e^- or the Bethe-Heitler process. Detailed simulations showed that from all background processes, which lead to correlated e^+e^- pairs, only the Dalitz decay of the ω mesons contributes appreciably in the e^+e^- mass region of interest. To simulate each physics process, a realistic model was employed and corrected for the CLAS acceptance. The events were generated using a code based on a semi-classical Boltzmann-Uehling-Uhlenbeck (BUU) transport model developed by the Giessen group that treats photon-nucleus reactions as a two-step process [94]. In the first step, the incoming photons react with a single nucleon, taking into account various nuclear effects, *e.g.* shadowing, Fermi motion, collisional broadening, Pauli blocking, and nuclear binding. Then, in the second step, the produced particles are propagated explicitly through the nucleus allowing for final state interactions, governed by the semi-classical BUU transport equations. A rather complete treatment of the e^+e^- pair production from γA reactions at Jefferson Lab energies using this

code can be found in Ref. [95].

Another source of background for the e^+e^- mass distributions, the combinatorial background, are events where the electron and the positron originate in uncorrelated processes within the same 2 ns wide CEBAF beam bucket. The most salient feature of the uncorrelated sources is that they produce same-charge lepton pairs as well as oppositely charged pairs. This is also true for the measurement of opposite-sign pions or muons for which the combinatorial method has also been used in the past [96, 97]. This method has also been used in the extraction of resonance signals [98] and proton femtoscopy of eA interactions [99]. The combinatorial background is determined by an event-mixing technique. The electrons of a given event are combined with positrons of another event, as the two samples of electrons and positrons are completely uncorrelated. This produces the phase-space distribution of the combinatorial background. This distribution was then normalized to the number of expected opposite-charge pairs, which unambiguously can be determined from same-charge pairs.

The experimental e^+e^- mass distributions are shown in Fig. 5 after subtraction of the combinatorial background. Also shown are BUU model calculations for various e^+e^- channels, fitted to the data, which describe the data very well. The narrow distributions of the ϕ and ω meson, including its Dalitz decay, are readily normalized to the data. The subtraction of these distributions results in the experimental spectra of the ρ mass shown in Fig. 6. The shape of the spectral function is well approximated by a Breit-Wigner function times a factor $1/\mu^3$, where μ is the mass of the e^+e^- pair [26]. Experimental values of the in-medium ρ mass and width are then obtained from fits to the data (solid curves). The in-medium widths of the ρ for the nuclear targets are slightly larger than the free value, *e.g.* $\Gamma = 218 \pm 15$ MeV for the Fe-Ti target, but are well understood as collisional broadening [100] as modeled in the BUU calculations. They are not compatible with the doubling of the ρ width reported by NA60 [82].

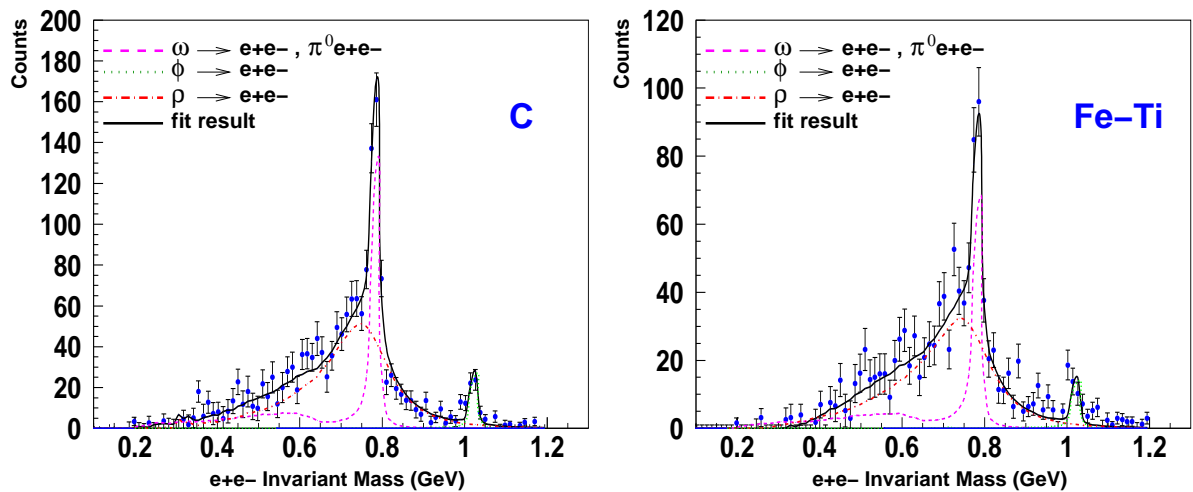


Figure 5. Experimental e^+e^- invariant mass distributions obtained for carbon (left panel) and Fe-Ti (right panel) after subtraction of the combinatorial background. The curves are calculations by the BUU model [101, 102] for various e^+e^- channels. Figures are from [25].

The observed in-medium ρ masses are consistent with the free value. The relative ρ -mass shift for the Fe-Ti target and ρ momenta ranging from 0.8 to 3.0 GeV is $\alpha = 0.02 \pm 0.02$. This is consistent with the predictions of no significant mass shift by the calculations of Ref. [77, 78] and those of Ref. [94, 103] at ρ vector meson momenta > 1 GeV. The total systematic uncertainty for the measured α due to various sources is estimated to be $\Delta\alpha = \pm 0.01$ [26]. The result from

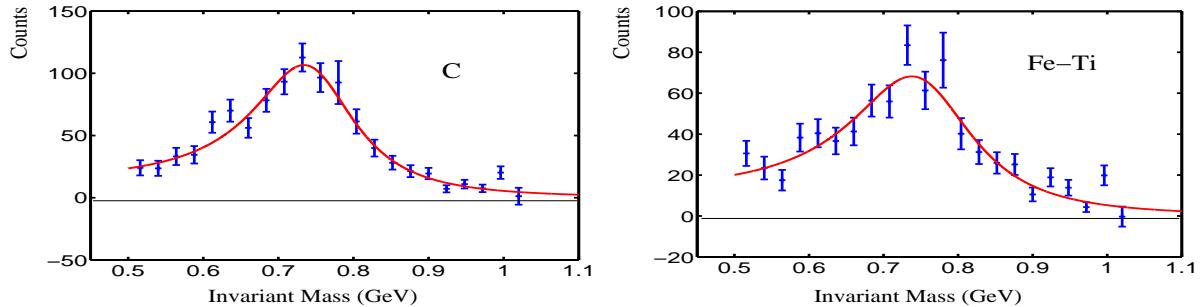


Figure 6. Extracted ρ mass spectra from the CLAS g7 run data for the C (left), and Fe-Ti (right panel) targets. The curves show fits of a Breit-Wigner function times $1/\mu^3$, where μ is the e^+e^- invariant mass. Figures are from [25].

the CLAS g7 run sets an upper limit of $\alpha = 0.04$ with a 95% confidence level. It does not favor the prediction of Refs. [1] and [73] for a 20% mass shift and $\alpha = 0.16 \pm 0.06$ respectively, and is significantly different from other similar experiments [85, 86, 87], where $\alpha = 0.092 \pm 0.002$, with no broadening in the width of the ρ meson. The g7 results are consistent with the result of a recent re-analysis of ω meson photoproduction data [89] which found broadening, but no mass shift, in the ω signal.

The extracted experimental ρ mass spectrum with the unique characteristic of electromagnetic interactions in both the production and decay is well described by the ρ functional form obtained from the exact calculations given in Refs. [95, 104, 105] with no modification beyond standard nuclear many-body effects. Recently, the dilepton spectra were calculated by Riek *et al.* [106, 107] within the same effective hadronic model that describes NA60 data [108] and found to be in good agreement with the CLAS data. With the availability of more sophisticated theoretical models and improved analysis techniques, future experiments with higher statistics are expected to make a conclusive statement about the momentum dependence of the in-medium modifications and the nature of the QCD vacuum.

4. Modification of partonic processes

A tremendous amount of progress has been achieved over the past decade in understanding the modification of partonic processes in the medium. New experiments at Fermilab, DESY, and Jefferson Lab have uncovered a wealth of new information on partonic processes in the *cold* nuclear medium through the Drell-Yan process and through semi-exclusive DIS. Experiments at RHIC have generated a strong interest in the same partonic processes in the *hot* medium through the observation of jet quenching, and these observations will soon be tested with much higher energies at the LHC [109]. The Jefferson Lab experiments [28, 110] in particular promise to uniquely measure spacetime properties of QCD inaccessible to any other experiments, with sufficient luminosity and kinematic reach to achieve a detailed understanding of the processes by which hadrons are formed and of the propagation of quarks both in the medium and in vacuum.

A primary aim of the measurements in the cold medium is to explicate the fundamental QCD processes involved in parton propagation and hadron formation. Particularly in the space-time domain, the well-understood properties of nuclei can be exploited to extract quantities such as the free quark lifetime (the so-called production time) and hadron formation times. In the process of confronting the data with model calculations, the detailed mechanisms of hadron formation can also be constrained and characterized. As a secondary benefit, the insight gained by these studies can in principle be used to better understand the data from the relativistic heavy

ion collisions. Much theoretical work is needed to actually accomplish this, however, there are examples of efforts to describe both the hot and cold matter within the same theoretical language [111, 112].

The following discussion centers around two primary interests. First, the modification of fragmentation functions is discussed. The primary observable, the hadronic multiplicity ratio, is a measure of the modification of the fragmentation functions. Through modeling it can be related to hadron formation lengths and fragmentation mechanisms. Second, the topic of quark energy loss is discussed. Here the primary observable is the broadening of the distributions in hadron transverse momentum. It is expected that the production time can be estimated from this variable within certain kinematic regions. Further, this observable can be connected to a variety of important and interrelated topics, such as partonic multiple scattering in the medium, energy loss *via* gluon bremsstrahlung, and jet quenching in relativistic heavy ion collisions. Recent reviews, with a more complete coverage of theoretical approaches, may be found in Refs. [113, 114].

4.1. Fragmentation functions

In the simplest picture, fragmentation functions $D_h^q(z)$ describe the probability that an energetic quark q or antiquark \bar{q} evolves into a specific hadron h , where the ratio of the hadron energy to the quark energy is $z = E_h/E_q$. They enter into the expression for the cross section for semi-inclusive electron scattering in combination with the parton distribution functions. A direct measure of the nuclear medium modification of the fragmentation functions is given by the *hadronic multiplicity ratio* R_M^h :

$$R_M^h(z, \nu, Q^2, p_T^2, \phi) = \frac{\left(\frac{N_h(z, \nu, Q^2, p_T^2, \phi)}{N_e^{DIS}(\nu)} \right)_A}{\left(\frac{N_h(z, \nu, Q^2, p_T^2, \phi)}{N_e^{DIS}(\nu)} \right)_D}, \quad (3)$$

where the numerator pertains to larger nucleus A , the denominator pertains to the deuterium nucleus D , and the variables not previously defined are p_T^2 , the hadron momentum transverse to the virtual photon direction squared, and ϕ , the azimuthal angle around the virtual photon direction of the electron-hadron scattering plane. This observable, from the parton model perspective, is determined by the parton distribution functions and the fragmentation functions in the two nuclei. Experimentally it is now known that the nuclear medium induces a strong z dependence on R_M^h , demonstrating that it is indeed the fragmentation functions that are modified, in addition to the much smaller changes in the parton distribution functions that are associated with the EMC effect.

While there were historical measurements of semi-inclusive hadron production on nuclear targets prior to the 1990's, the first measurements that included identification of the produced hadrons were those of the HERMES experiment at DESY. These pioneering measurements established the basic features of the multiplicity ratio:

- suppression of R_M^h at high z and at low ν that systematically increases for larger nuclei;
- an enhancement of R_M^h at high p_T^2 in analogy with the Cronin effect seen in $p - A$ collisions;
- R_M^h depends on the hadron species produced.

The Jefferson Lab 5 GeV experiment, while more limited in kinematic reach than the HERMES experiment, has been able to observe qualitatively new behavior due to the much higher Jefferson Lab luminosity and the capacity for accommodating solid targets, thus probing

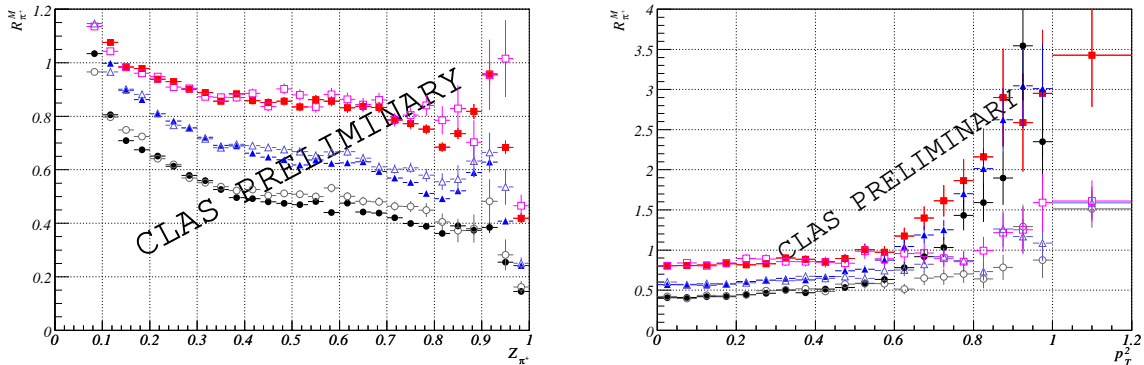


Figure 7. Preliminary data for the CLAS hadronic multiplicity ratio measurement as a function of z_{π^+} (upper plot) and p_T^2 (lower plot). The data shown are for positive pions for carbon (squares), iron (triangles), and lead (circles) targets normalized to a deuterium target. The data with filled (open) symbols correspond to the range $\nu = 2.2 - 3.2$ ($3.2 - 3.7$) GeV and $Q^2 = 1.0 - 1.3$ GeV². The errors shown are statistical only. See Refs. [115, 116] for more discussion of the preliminary results for positive pions, and Ref. [117] for preliminary results for neutral kaons.

the largest nuclei. Because the Jefferson Lab data have two orders of magnitude more integrated luminosity, it is possible to bin the data in up to three kinematic variables while preserving good statistical accuracy. Thus, a fuller exploration of the kinematic dependence of R_M^h is possible. A second consequence of the higher luminosity is access to production of rarer hadrons, such as K^0 , η , and potentially η' , as well as exploratory studies with baryons such as protons, Λ s and Σ s. This complements the HERMES data set, in which the RICH detector was able to identify K^+ and K^- as well as antiprotons; both experiments have access to the three pion charge states, which provides a good cross-check to validate the consistency of the two data sets. Figure 7 shows a small subset of the preliminary Jefferson Lab data for R_M^h for positive pions. It can be seen from this figure that the basic dependencies established by the HERMES data are well reproduced by these lower energy data (suppression at high z , enhancement at high p_T^2), and are extended to the heaviest nuclei and to three-fold differential distributions (ν , Q^2 , and z in the upper panel, and ν , Q^2 , and p_T^2 in the lower panel). In addition to these studies for positive pions, preliminary results for neutral kaons can be found in Ref. [117], and studies are underway for neutral pions and η [118], negative pions, protons, and positive kaons [119], and Λ and Σ baryons. These types of studies lay the groundwork for future experiments at high luminosity facilities [110, 120].

To interpret these data and extract the physics of interest, a model is needed. Many models have been constructed to describe the HERMES results, and a number of these are now being used to address the new Jefferson Lab data. Existing models fall into three classes. First, there are models which assume that hadron formation only takes place outside the nucleus, and then use a pQCD framework to describe the interaction of a moving parton with the medium. In this picture, the behavior of R_M^h is due entirely to the stimulated emission of gluons resulting from partonic multiple scattering. The second class of models invokes hadron formation within the medium as the primary cause of the behavior of R_M^h , such that the semi-classical interaction of a forming hadron (or ‘prehadron’) removes flux from the observed final state channel through hadronic interactions. The third class of model has emerged only recently; it retains ingredients from the other two approaches, but treats the interaction in a

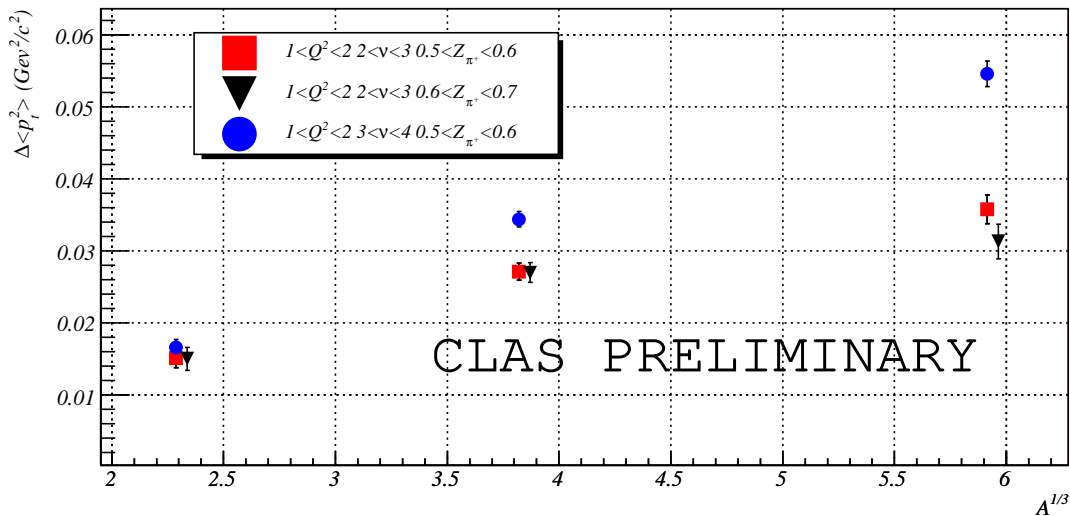


Figure 8. Mass number dependence of p_T -broadening in nuclear DIS. CLAS preliminary data for positive pions for carbon, iron, and lead targets three-fold differential in Q^2 , ν , and z_{π^+} as shown in the legend. The errors shown are statistical only. See Refs. [115, 116] for more discussion of the preliminary results for positive pions, and Ref. [117] for preliminary results for neutral kaons.

fully quantum-mechanical framework. In this last approach an interference is observed between hadron formation inside the medium and outside the medium, and this gives rise to a non-trivial modification of R_M^h .

It is likely that the stringent constraints imposed by the new Jefferson Lab data will soon clarify what the essential model ingredients are. In particular, it is crucial to establish the relative importance of the two processes of gluon bremsstrahlung and prehadron interactions in describing the kinematic and flavor dependencies of R_M^h , and to understand the role of quantum interference in these processes. At that point it will be feasible to fully analyze the data from the 5 GeV data and from the planned 12 GeV Jefferson Lab Experiment E12-06-117, extracting hadron formation lengths from a variety of produced hadrons and constraining the mechanisms involved in their formation.

4.2. Quark energy loss

Quarks passing through a strongly-interacting medium are expected to lose energy through the medium-stimulated emission of gluons. This topic underwent intensive theoretical study by a number of groups beginning in the 1990's (see [121, 113]). Experimentally this topic was a focus of the Fermilab Drell-Yan experiments [122] as well as a phenomenon invoked to explain the jet quenching observed at RHIC. Extraction of a reliable value for the quark energy loss has proven to be an elusive goal, and estimated values from both theoretical and experimental work have varied by more than one order of magnitude.

While obtaining a quantitative value for quark energy loss is still a challenge, there are closely related parameters that are now accessible through experiment. Principal among these is the *transport coefficient* \hat{q} , which quantifies the transverse momentum accumulated by the quark per unit path length. This parameter or its equivalent appears in every calculation of quark energy loss for cold and hot matter and thus measuring it is of high interest. Using the BDMPS

formalism [123, 124] for the following discussion, the transport coefficient is related to the mean transverse momentum acquired by quark q along a trajectory of length L :

$$\langle p_{T,q}^2 \rangle = \hat{q}L, \quad (4)$$

and the radiative energy loss is given by

$$-\frac{dE}{dz} = \frac{1}{4}\alpha_s N_c \hat{q}L, \quad (5)$$

where α_s is the strong coupling constant and N_c is the number of colors. These equations, while specific to one theoretical approach, demonstrate the close connection between energy loss, p_T broadening, and the transport coefficient.

As with the quark energy loss, there is an order of magnitude spread among the theoretical and experimental estimates for \hat{q} . For example, an estimate from pQCD is the following:

$$\hat{q} = \frac{4\pi^2 \alpha_s C_R}{N_c^2 - 1} \rho x G(x, Q^2), \quad (6)$$

where C_R is the SU(3) color charge of the parton, equal to $(N_c^2 - 1)/2N_c$ and N_c for quarks and gluons respectively, x is the Bjorken scaling variable, ρ is the nuclear medium density, and G is the gluon density in the nucleon. The connection between gluon density and \hat{q} is a consistent theme among the various theoretical approaches.

The new precision Jefferson Lab and HERMES data from the past decade will provide a definitive measurement of unprecedented precision for the value of \hat{q} in cold nuclear matter. In this case, the experimentally measured hadron observable $\Delta p_{T,h}^2$ is very closely related to \hat{q} and rather minor assumptions are required to derive it from the data.

A related exercise is the extraction of the lifetime of the free quark, referred to as the ‘production time’ τ_p , from the data. Although heuristic estimates of this quantity can be found, it has never been measured experimentally. While an exact form is not known, its general dependence on ν and z is expected to be of the form

$$\tau_p \approx z(1 - z)\nu, \quad (7)$$

based on energy conservation and special relativity.

The Jefferson Lab data suggest that a unique window exists for measuring τ_p where the production length τ_p/c is comparable to nuclear dimensions. In this regime, interactions with the nucleus allow a determination of τ_p , while at higher ν the quark hadronizes outside the nucleus and no information on its lifetime can be gained. The method of extraction makes use of the p_T broadening, which occurs during the phase in which the quark is propagating as a colored object. Once it undergoes color neutralization and becomes a prehadron, its interactions with the nucleus contribute much less broadening per unit path length. Thus, when the quark’s color is neutralized, the broadening essentially stops. This is manifested experimentally by a non-linear saturation in the relationship between Δp_T and the nuclear size $\approx A^{\frac{1}{3}}$.

Figure 8 shows a small subset of the preliminary Jefferson Lab 5 GeV data for three different three-dimensional bins in Q^2 , ν , and z . On the vertical axis is the experimentally observed p_T broadening, $\Delta p_{T,h}^2$. On the horizontal axis is $A^{\frac{1}{3}}$ which is proportional to the average medium thickness for the three nuclei shown. It is seen that these data exhibit the non-linear saturation described above, in varying degrees. To interpret these in terms of quark degrees of freedom one must correct the hadron’s $\Delta p_{T,h}^2$ to the value of the quark-level $\Delta p_{T,q}^2$, typically using a simple kinematic multiplier. If the prescription of Domdey *et al.* [125] is used for this, one finds that the data shown in this figure follow the behavior expected from Eq. (7) above. A detailed study

of the full data set is underway, but it is already evident that there is qualitative confirmation of the physical picture and a clear path to extracting the free quark lifetime τ_p from these data.

The determination of τ_p provides a precise value of L in Eq. (4), and the value of the quark-level $\Delta p_{T,q}^2$ gives the quantity on the left-hand side of this equation, thus determining \hat{q} . This can then be used to estimate the quark energy loss through Eq. (5).

In principle, the quark energy loss can also be determined from a direct measurement using the same data and comparing the energy spectra of leading hadrons emerging from nuclei of different thicknesses. Careful consideration of Fermi motion and nuclear pion production are required to extract a direct estimate. An evaluation of these possibilities is also underway.

5. Summary

In this article we have reviewed the tremendous successes of Jefferson Lab experiments that aimed at the understanding of in-medium modifications of hadron properties and quark interactions over the last decade. Particularly, we have highlighted three experiments: First, the $^4\text{He}(\vec{e}, e'\vec{p})^3\text{H}$ polarization transfer measurements revealed possible medium modifications of the bound proton electromagnetic form factors. Second, the study of vector meson photoproduction on nuclei has observed no mass shift of the ρ meson in the nuclear medium and a width consistent with expected collision broadening. These results put tight constraints on models of in-medium hadron properties. Finally, in-medium modification of fragmentation function ratios extracted in Jefferson Lab with high statistics and accuracy, has opened new experimental possibilities that connect to the future Jefferson Lab 12 GeV upgrade. The data analysis of some more recent experiments to study the Coulomb sum rule or the nuclear EMC effect are underway and exciting results from those are expected to come out soon.

Acknowledgments

Notice: Authored by Jefferson Science Associates, LLC under U.S. DOE Contract No. DE-AC05-06OR23177. The U.S. Government retains a non-exclusive, paid-up, irrevocable, worldwide license to publish or reproduce this manuscript for U.S. Government purposes. We would like to thank C. Djali and J. Arrington for useful discussions about this work. S.S. acknowledges support from the U.S. National Science Foundation, NSF PHY-0856010. W.K.B. acknowledges support from CONICYT grant number 1080564.

References

- [1] G. E. Brown and M. Rho, *Phys. Rev. Lett.* **66**, 2720 (1991).
- [2] S. R. Beane, P. F. Bedaque, K. Orginos and M. J. Savage, *Phys. Rev. Lett.* **97**, 012001 (2006); N. Ishii, S. Aoki and T. Hatsuda, *Phys. Rev. Lett.* **99**, 022001 (2007).
- [3] S. R. Beane, P. F. Bedaque, T. C. Luu, K. Orginos, E. Pallante, A. Parreno and M. J. Savage, *Nucl. Phys.* **A794**, 62 (2007); H. Nemura, N. Ishii, S. Aoki and T. Hatsuda, *Phys. Lett. B* **673**, 136 (2009).
- [4] K. Saito, K. Tsushima and A. W. Thomas, *Prog. Part. Nucl. Phys.* **58**, 1 (2007).
- [5] R.P. Bickerstaff and A.W. Thomas, *J. Phys. G* **15**, 1523 (1989); M. Arneodo, *Phys. Rep.* **240**, 301 (1994); D. F. Geesaman, K. Saito and A. W. Thomas, *Annu. Rev. Nucl. Part. Sci.* **45**, 337 (1995); G. Piller and W. Weise, *Phys. Rep.* **330**, 1 (2000).
- [6] G.A. Miller and J.R. Smith, *Phys. Rev. C* **65**, 015211 (2002); *Phys. Rev. C* **66**, 049903(E) (2002); J.R. Smith and G.A. Miller, *Phys. Rev. C* **65**, 055206 (2002).
- [7] J.R. Smith and G.A. Miller, *Phys. Rev. Lett.* **91**, 212301 (2003).
- [8] K. J. Eskola, V. J. Kolhinen and C. A. Salgado, *Eur. Phys. J. C* **9**, 61 (1999); K. J. Eskola, V. J. Kolhinen and P. V. Ruuskanen, *Nucl. Phys.* **B535**, 351 (1998).
- [9] M. Hirai, S. Kumano and M. Miyama, *Phys. Rev. D* **64**, 034003 (2001).
- [10] Jefferson Lab Experiment E89-008, D. Day and B. Filippone, co-spokespersons.
- [11] Jefferson Lab Experiment E02-019, A. Lung, J. Arrington, D. Day and B. Filippone, co-spokespersons.
- [12] Jefferson Lab Experiment E03-103, J. Arrington and D. Gaskell, co-spokespersons.
- [13] J. Seely *et al.*, *Phys. Rev. Lett.* **103**, 202301 (2009).
- [14] Jefferson Lab Experiment E99-118, A. Bruell, J. Dunne and C. Keppel, co-spokespersons.

- [15] Jefferson Lab Experiment E04-001, A. Bodek and C. Keppel, co-spokespersons.
- [16] Jefferson Lab Experiment E89-033, C. Chang, C. Glashauser, S. Nanda and P. Rutt, co-spokespersons.
- [17] S. Malov *et al.*, Phys. Rev. C **62**, 057302 (2000).
- [18] S. Dieterich *et al.*, Phys. Lett. B **500**, 47 (2001).
- [19] Jefferson Lab Experiment E93-049, R. Ent and P. Ulmer, co-spokespersons.
- [20] Jefferson Lab Experiment E03-104, R. Ent, R. Ransome, S. Strauch and P. Ulmer, co-spokespersons.
- [21] S. Strauch *et al.*, Phys. Rev. Lett. **91**, 052301 (2003).
- [22] M. Paolone *et al.*, Phys. Rev. Lett. **105**, 072001 (2010).
- [23] Jefferson Lab Experiment E05-110, J.-P. Chen, S. Choi and Z.-E. Meziani, co-spokespersons.
- [24] Jefferson Lab Experiment E01-112, C. Djalali, M. Kossov and D. Weygand, co-spokespersons.
- [25] R. Nasseripour *et al.*, Phys. Rev. Lett. **99** 262302 (2007).
- [26] M. H. Wood, *et al.*, Phys. Rev. C **78** 015201 (2008).
- [27] Jefferson Lab Experiment E89-028, J. Finn and P. Ulmer, co-spokespersons.
- [28] Jefferson Lab Experiment E02-104, W. Brooks, spokesperson.
- [29] S. A. Moszkowski and B. L. Scott, Ann. Phys. (Paris) **11**, 65 (1960).
- [30] D. H. Lu *et al.*, Phys. Lett. B **417**, 217 (1998); Phys. Rev. C **60**, 068201 (1999).
- [31] M. R. Frank, B. K. Jennings and G. A. Miller, Phys. Rev. C **54**, 920 (1996).
- [32] U. T. Yakhshiev, U.-G. Meissner, and A. Wirzba, Eur. Phys. J. A **16**, 569 (2003).
- [33] J. R. Smith and G. A. Miller, Phys. Rev. C **70**, 065205 (2004).
- [34] T. Horikawa and W. Bentz, Nucl. Phys. **A762**, 102 (2005).
- [35] W. Wen and H. Shen, Phys. Rev. C **77**, 065204 (2008).
- [36] D. H. Lu, A. W. Thomas and K. Tsushima, arXiv:nucl-th/0112001; K. Tsushima, H.-C. Kim and K. Saito, Phys. Rev. C **70**, 038501 (2004).
- [37] S. Liuti, arXiv:hep-ph/0601125v2.
- [38] V. Guzey, A. W. Thomas and K. Tsushima, Phys. Lett. B **673**, 9 (2009).
- [39] V. Guzey, A. W. Thomas and K. Tsushima, Phys. Rev. C **79**, 055205 (2009).
- [40] W. Melnitchouk, K. Tsushima and A. W. Thomas, Eur. Phys. J. A **14**, 105 (2002).
- [41] I. Sick, in *Proc. Int. Conf. on Weak and Electromagnetic Interactions in Nuclei*, ed. H. Klapdor (Springer-Verlag, Berlin, 1986) p. 415.
- [42] J. Jourdan, Phys. Lett. B **353**, 189 (1995).
- [43] R. G. Arnold, C. E. Carlson and F. Gross, Phys. Rev. C **23**, 363 (1981).
- [44] D. Eyl *et al.*, Z. Phys. A **352**, 211 (1995).
- [45] B. D. Milbrath and J. McIntyre *et al.*, Phys. Rev. Lett. **80**, 452 (1998).
- [46] D. H. Barkhuff *et al.*, Phys. Lett. B **470**, 39 (1999).
- [47] B. Hu *et al.*, Phys. Rev. C **73**, 064004 (2006).
- [48] J. M. Laget, Nucl. Phys. **A579**, 333 (1994).
- [49] J. M. Udias *et al.*, Phys. Rev. Lett. **83**, 5451 (1999); J. A. Caballero, T. W. Donnelly, E. Moya de Guerra and J. M. Udias, Nucl. Phys. **A632**, 323 (1998).
- [50] J. M. Udias and J. R. Vignote, Phys. Rev. C **62**, 034302 (2000).
- [51] A. Meucci, C. Giusti and F. D. Pacati, Phys. Rev. C **66**, 034610 (2002).
- [52] T. de Forest, Nucl. Phys. **A392**, 232 (1983).
- [53] J. A. McNeil, L. Ray and S. J. Wallace, Phys. Rev. C **27**, 2123 (1983).
- [54] R. J. Woo *et al.*, Phys. Rev. Lett. **80**, 456 (1998).
- [55] J. Gao *et al.*, Phys. Rev. Lett. **84**, 3265 (2000).
- [56] R. Schiavilla *et al.*, Phys. Rev. Lett. **94**, 072303 (2005).
- [57] P. Lava *et al.*, Phys. Rev. C **71**, 014605 (2005).
- [58] S. P. Malace, M. Paolone and S. Strauch, AIP Conf. Proc. **1056**, 141 (2008).
- [59] S. P. Malace *et al.*, Phys. Rev. Lett. **106**, 052501 (2011).
- [60] J. Morgenstern and Z.-E. Meziani, Phys. Lett. B **515**, 269 (2001).
- [61] K. Saito, K. Tsushima and A. W. Thomas, Phys. Lett. B **465**, 27 (1999).
- [62] J. Carlson, J. Jourdan, R. Schiavilla and I. Sick, Phys. Lett. B **553**, 191 (2003).
- [63] G.A. Miller, Eur. Phys. J. A **31**, 578 (2007).
- [64] J. Arrington, J. Phys. Conf. Ser. **69**, 012024 (2007).
- [65] J. Gomez *et al.*, Phys. Rev. D **49**, 4348 (1994).
- [66] J. Arrington *et al.*, Phys. Rev. C **73**, 035205 (2006).
- [67] V. Tvaskis *et al.*, Phys. Rev. Lett. **98**, 142301 (2007).
- [68] I. C. Cloet, W. Bentz, A. W. Thomas, Phys. Rev. Lett. **95**, 052302 (2005); Phys. Lett. B **642**, 210 (2006).
- [69] Jefferson Lab Letter of Intent LOI-06-003, V. Dharmawardane, contact person.
- [70] Jefferson Lab Letter of Intent LOI-06-004, X. Zheng and A. Deur, contact persons.

- [71] O. A. Rondon, Phys. Rev. C **60**, 035201 (1999).
- [72] K. Saito, M. Ueda, K. Tsushima and A. W. Thomas, Nucl. Phys. **A705**, 119 (2002).
- [73] T. Hatsuda and S. H. Lee, Phys. Rev. C **46**, 34 (1992).
- [74] M. Herrman *et al.*, Nucl. Phys. **A545**, 267c (1992).
- [75] R. Rapp *et al.*, Nucl. Phys. **A617**, 472 (1997).
- [76] W. Peters, M. Post, H. Lenske, S. Leupold and U. Mosel, Nucl. Phys. **A632**, 109 (1997).
- [77] M. Urban *et al.*, Nucl. Phys. **A673**, 357 (2000).
- [78] D. Cabrera *et al.*, Nucl. Phys. **A705**, 90 (2002).
- [79] M. F. M. Lutz *et al.*, Nucl. Phys. **A706**, 431 (2002).
- [80] F. Eichstaedt *et al.*, nucl-th/07040154.
- [81] D. Adamova *et al.*, nucl-ex/0611022.
- [82] R. Arnaldi *et al.*, Phys. Rev. Lett. **96**, 162302 (2006).
- [83] S. Damjanovic *et al.*, Eur. Phys. J. C **49**, 235 (2007).
- [84] S. Damjanovic *et al.*, Nucl. Phys. **A783**, 327 (2007).
- [85] R. Muto *et al.*, J. Phys. G: Nucl. Part. Phys. **30**, 1023 (2004).
- [86] R. Muto *et al.*, Phys. Rev. Lett. **98**, 042501 (2007).
- [87] M. Naruki *et al.*, Phys. Rev. Lett. **96**, 092301 (2006).
- [88] D. Trnka *et al.*, Phys. Rev. Lett. **94**, 192303 (2005).
- [89] M. Nanova *et al.*, arXiv:1005.5694 [nucl-ex].
- [90] K. Tsushima, D. H. Lu, A. W. Thomas and K. Saito, Phys. Lett. B **443**, 26 (1998).
- [91] R. S. Hayano, S. Hirenzaki and A. Gillitzer, Eur. Phys. J. A **6**, 99 (1999).
- [92] K. Saito, K. Tsushima, D. H. Lu and A. W. Thomas, Phys. Rev. C **59**, 1203 (1999).
- [93] B. A. Mecking *et al.*, Nucl. Instr. Meth. A **503**, 513 (2003).
- [94] P. Muehlich, T. Falter, C. Greiner, J. Lehr, M. Post and U. Mosel, Phys. Rev. C **67**, 024605 (2003).
- [95] M. Effenberger, E.L. Bratkovskaya and U. Mosel, Phys. Rev. C **60**, 044614 (1999).
- [96] G. Jancso *et al.*, Nucl. Phys. **B124**, 1 (1977).
- [97] D. Jouan *et al.*, Internal Report, Institut de Physique Nucleaire d'Orsay, IPNO-DR-02.015 (2002).
- [98] D. Drijard, H. G. Fischer and T. Nakada, Nucl. Inst. Meth. **225**, 367 (1984).
- [99] A. V. Stavinsky *et al.*, Phys. Rev. Lett. **93**, 192301 (2004).
- [100] D. V. Bugg, Nucl. Phys. **B88**, 381 (1975).
- [101] M. Effenberger and U. Mosel, Phys. Rev. C **62**, 014605 (2000).
- [102] M. Effenberger, E. L. Bratkovskaya, W. Cassing and U. Mosel, Phys. Rev. C **60**, 027601 (1999).
- [103] M. Post, S. Leupold and U. Mosel, Nucl. Phys. **A741**, 81 (2004). Phys. Rev. C **63**, 015204 (2001).
- [104] G.-Q. Li, C. M. Ko, G. E. Brown and H. Sorge, Nucl. Phys. **A611**, 539 (1996).
- [105] H. B. O'Connell *et al.*, Prog. Part. Nucl. Phys. **39**, 201 (1997).
- [106] F. Riek, R. Rapp, T.-S.H. Lee, Yongseok Oh, Phys. Lett. B **677**, 116 (2009).
- [107] F. Riek, R. Rapp, Yongseok Oh, and T.-S.H. Lee, Phys. Rev. C **82**, 015202 (2010).
- [108] H. van Hees and R. Rapp, Nucl. Phys. A **806**, 339 (2008).
- [109] W. K. Brooks, AIP Conf. Proc. **1265**, 276 (2010).
- [110] Jefferson Lab Experiment E12-06-117, W. Brooks, G. Gilfoyle, K. Hafidi, K. Hicks, M. Holtrop, K. Joo, G. Niculescu and M. Wood, co-spokespersons.
- [111] A. Majumder and B. Müller, Phys. Rev. C **77**, 054903 (2008).
- [112] A. Majumder, R. J. Fries and B. Müller, Phys. Rev. C **77**, 065209 (2008).
- [113] A. Accardi, F. Arleo, W. K. Brooks, D. D'Enterria, and V. Muccifora, Riv. Nuov. Cim. **09**, 439 (2009).
- [114] A. Majumder and M. van Leeuwen, arXiv:1002.2206v3 [hep-ph].
- [115] H. Hakobyan, PhD thesis, Yerevan State University (2008).
- [116] W. K. Brooks and H. Hakobyan, AIP Conf. Proc. **1056**, 215 (2008), Nucl. Phys. **A830**, 361c (2009), AIP Conf. Proc. **1265**, 230 (2010).
- [117] K. Hicks and A. Daniel, arXiv:0907.5362v1 [nucl-ex].
- [118] T. Mineeva, W. K. Brooks, K. Joo and M. Ungaro, Bull. Amer. Phys. Soc. **54**, Number 10, <http://meetings.aps.org/link/BAPS.2009.HAW.EF.12> (2009).
- [119] R. Dupre and K. Hafidi, Bull. Amer. Phys. Soc. **55**, Number 1, <http://meetings.aps.org/link/BAPS.2010.APR.S8.9> (2010).
- [120] W. K. Brooks, PoS DIS2010, 258 (2010).
- [121] R. Baier, D. Schiff and B. G. Zakharov, Annu. Rev. Nucl. Part. Sci. **50**, 37 (2000).
- [122] M. J. Leitch *et al.*, Phys. Rev. Lett. **84**, 3256 (2000).
- [123] R. Baier, Y. L. Dokshitzer, A. H. Mueller, S. Peigne and D. Schiff, Nucl. Phys. **B484**, 265 (1997).
- [124] R. Baier, Y. L. Dokshitzer, A. H. Mueller and D. Schiff, Nucl. Phys. **B531**, 403 (1998).
- [125] S. Domdey, D. Grunewald, B. Z. Kopeliovich and H. J. Pirner, Nucl. Phys. **A825**, 200 (2009).